Time-Varying Multicomponent Signal Modeling for Analysis of Surface EMG Data

Miroslav Zivanovic

***Abstract*—We present a novel approach to surface EMG data characterization by using time-varying multicomponent signal modeling. An EMG signal is described as a set of stationary non-harmonically related sinusoids (signal components) whose time-varying bandwidth is modeled by polynomials. The polynomial coefficients, estimated from a set of linear equations, capture the relationship between the instantaneous frequency and amplitude for individual signal components. It is proposed that such a compact EMG signal modeling may be a good candidate for a number of applications in surface electromyography: compression, muscle activity detection and low-bias conduction velocity, to name a few.**

***Index Terms*—Multicomponent signals, non-stationary signals, signal modeling, surface electromyography.**

I. Introduction

In a number of surface electromyography signal processing applications there is a strong need for a compact description of time waveforms from the input signal recorded during contractions. Such applications typically include signal compression, classification, muscle fatigue characterization, and EMG-based speech recognition, among others.

The usual approach to parametric EMG signal characterization is based on statistical modeling of time-series, where an EMG signal is assumed to be the output of a stochastic process driven by the physiological properties of the muscle and the form of the contraction [1]. Accordingly, the dynamic of EMG signals is modeled as a linear autoregressive (AR) process, also known as an all-pole filter, whose output captures the EMG signal's statistical properties according to some goodness measure [2]–[13]. The AR approach has been used in applications like fatigue analysis and speech recognition. The non-parametric EMG signal characterization approach (transform-based methods) is based on signal decomposition into carefully chosen basis functions so that the input signal waveform is reconstructed with a minimum number of transform coefficients and distortion. The most popular of all is the discrete wavelet transform (DWT), which fits the signal to the set of scaled and delayed versions of a prototype function (mother wavelet). The DWT coefficients thus provide a multiscale representation from which the input signal can be synthesized. The methods grounded on the DWT have been used in EMG signal compression [14]–[16].

In this letter we propose a novel approach to EMG signal description based on multicomponent time-varying signal modeling. This approach has been successfully used in speech and music signal processing, where pitched signals are modeled as a set of harmonically related non-stationary sinusoids [17]–[19]. By dropping the harmonicity constraint, we conceive a surface electromyogram as a collection of non-harmonic sinusoids whose instantaneous amplitude and frequency vary over time. Those variations are captured by polynomials, whose coefficients describe the relationship between the time-varying amplitude and frequency modulation of the sinusoids in the analysis window. The signal model identification (parameter estimation) is rather straightforward as it boils down to solving a system of linear equations. Potential benefits of the proposed EMG signal model for surface EMG may come from applications like signal compression, onset/offset detection and mean conduction velocity estimation, as discussed in the last section of the present letter.

II. Method

A. EMG Signal Model

EMG signals are often treated as band-pass random signals whose energy is localized typically between 10–400 Hz [20]. The spectrum of such signals exhibits a series of peaks (local maxima) whose number and distribution is determined by the corresponding stochastic process and the analysis window. We can assume that each spectral peak represents an underlying sinusoid whose instantaneous frequency and amplitude determine the frequency spread (bandwidth) around the local maximum [21]. Fig. 1 shows a short segment of an EMG recording together with its Hanning windowed spectrum. Accordingly, the EMG signal $x(t)$ can be approximated as a K-component time-varying model $\hat{x}(t)$:

$$\hat{x}(t) = \sum_{k=1}^{K} A_k(t) \cos\left(2\pi f_k(t) t + \theta_k\right), \tag{1}$$

where $A_k(t)$ and $f_k(t)$ are the instantaneous amplitude and frequency respectively. Expression (1) can be rewritten in a more convenient way as:

$$\hat{x}(t) = \sum_{k=1}^{K} a_k(t) \sin\left(2\pi f_k(t) t\right) + b_k(t) \cos\left(2\pi f_k(t) t\right), \tag{2}$$

$$a_k(t) = -A_k(t) \sin\theta_k, b_k(t) = A_k(t) \cos\theta_k. \tag{3}$$

Manuscript received March 21, 2014; revised March 24, 2014; accepted March 24, 2014. Date of publication March 26, 2014; date of current version April 02, 2014. The associate editor coordinating the review of this manuscript and approving it for publication was Prof. Peter K. Willett.

The author is with the Electrical Engineering Department, Public University of Navarra, 31006 Pamplona, Spain (e-mail: miro@unavarra.es).

Color versions of one or more of the figures in this paper are available online at http://ieeexplore.ieee.org.

Digital Object Identifier 10.1109/LSP.2014.2313880

1070-9908 © 2014 IEEE. Personal use is permitted, but republication/redistribution requires IEEE permission.
See http://www.ieee.org/publications_standards/publications/rights/index.html for more information.

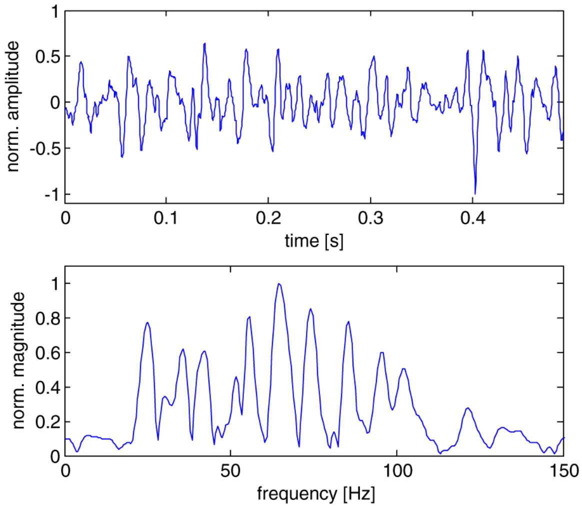

Fig. 1. An EMG time waveform (above) and its spectrum (below) where each peak represents an underlying time-varying sinusoid.

In (2) the unknown parameters $a_k(t)$, $b_k(\mathrm{t})$ and $f_k(t)$ need to be estimated. For N measurement points $t = t_1 \dots t_N$ expression (2) becomes an N-dimensional linear system with $3NK$ unknowns. Such a system cannot be solved; however, we can assume that in the analysis window the time-variations of $a_k(t)$, $b_k(\mathrm{t})$ and $f_k(t)$ are continuous, and therefore can be approximated by the following time polynomials for $k = 1 \dots K$:

$$a_k(t) = a_0^{(k)} + a_1^{(k)} t + a_2^{(k)} t^2 + \dots + a_M^{(k)} t^M = \sum_{m=0}^{M} a_m^{(k)} t^m, \tag{4}$$

$$b_k(t) = b_0^{(k)} + b_1^{(k)} t + b_2^{(k)} t^2 + \dots + b_M^{(k)} t^M = \sum_{m=0}^{M} b_m^{(k)} t^m, \tag{5}$$

$$f_k(t) = f_0^{(k)} + f_1^{(k)} t + f_2^{(k)} t^2 + \dots + f_M^{(k)} t^M = \sum_{m=0}^{M} f_m^{(k)} t^m. \tag{6}$$

By inserting (4)–(6) into (2) we obtain:

$$\hat{x}(t) = \sum_{k=1}^{K} \sum_{m=0}^{M} a_m^{(k)} t^m \sin(\lambda_k(t)) + \sum_{m=0}^{M} b_m^{(k)} t^m \cos(\lambda_k(t)), \tag{7}$$

$$\lambda_k(t) = 2\pi \left(f_0^{(k)} t + \sum_{m=1}^{M} f_m^{(k)} t^{m+1} \right), k = 1 \dots K. \tag{8}$$

The argument $\lambda_k(t)$ is written as a sum of the stationary (linear) and non-stationary (non-linear) frequency contribution, which can be analytically separated by transforming the sine and cosine in (7). For the kth component we have:

$$\begin{aligned} \sin(\lambda_k(t)) = \sin\left(2\pi f_0^{(k)} t\right) \cos\left(2\pi \sum_{m=1}^{M} f_m^{(k)} t^{m+1}\right) \\ + \cos\left(2\pi f_0^{(k)} t\right) \sin\left(2\pi \sum_{m=1}^{M} f_m^{(k)} t^{m+1}\right), \end{aligned} \tag{9}$$

$$\begin{aligned} \times \cos(\lambda_k(t)) = \cos\left(2\pi f_0^{(k)} t\right) \cos\left(2\pi \sum_{m=1}^{M} f_m^{(k)} t^{m+1}\right) \\ - \sin\left(2\pi f_0^{(k)} t\right) \sin\left(2\pi \sum_{m=1}^{M} f_m^{(k)} t^{m+1}\right). \end{aligned} \tag{10}$$

Furthermore, we can assume that for a short-time analysis the non-stationary trigonometric terms in (9) and (10) can be approximated by a single-term Taylor series:

$$\cos\left(2\pi \sum_{m=1}^{M} f_m^{(k)} t^{m+1}\right) \approx 1, \tag{11}$$

$$\sin\left(2\pi \sum_{m=1}^{M} f_m^{(k)} t^{m+1}\right) \approx 2\pi \sum_{m=1}^{M} f_m^{(k)} t^{m+1}. \tag{12}$$

By combining (9)–(12) we can rewrite (8) as:

$$\hat{x}(t) = \sum_{k=1}^{K} s_k(t) \sin\left(2\pi f_0^{(k)} t\right) + c_k(t) \cos\left(2\pi f_0^{(k)} t\right), \tag{13}$$

$$s_k(t) = \sum_{i=0}^{2M+1} \left[a_i^{(k)} - 2\pi \sum_{m=0}^{i-2} b_m^{(k)} f_{i-m-1} \right] t^i = \sum_{i=0}^{2M+1} s_i^{(k)} t^i, \tag{14}$$

$$c_k(t) = \sum_{i=0}^{2M+1} \left[b_i^{(k)} + 2\pi \sum_{m=0}^{i-2} a_m^{(k)} f_{i-m-1} \right] t^i = \sum_{i=0}^{2M+1} c_i^{(k)} t^i. \tag{15}$$

Expressions (13)–(15) represent the EMG time-varying multicomponent signal model, in which all the non-stationarities are captured by the $2M+1$–order polynomials $s_k(t)$ and $c_k(t)$. The model is linear-in-parameters and therefore the polynomial coefficients $s_i^{(k)}$ and $c_i^{(k)}$ can be easily obtained by solving a linear system of equations. The internal structure of these coefficients, given by (14) and (15), shows the relationship between the instantaneous amplitude and frequency and allow for estimating $a_k(t)$, $b_k(\mathrm{t})$ and $f_k(t)$, if a specific application demands it.

B. Model Parameter Estimation

In order to estimate the polynomial coefficients $s_i^{(k)}$ and $c_i^{(k)}$ we shall proceed by minimizing the following cost function at N measurement points:

$$\sum_{n=1}^{N} |x(t_n) - \hat{x}(t_n)|^2, \tag{16}$$

For the sake of simplicity, let us pose the estimation problem in the matrix form:

$$\mathbf{x} = \hat{\mathbf{x}} + \mathbf{e} = \mathbf{\Phi} \boldsymbol{\theta} + \mathbf{e}, \tag{17}$$

where the vectors $\mathbf{x}$ and $\hat{\mathbf{x}}$ contain the samples of the input signal and model respectively, while $\mathbf{e}$ represents the modeling errors. The vector $\boldsymbol{\theta}$ contains the polynomial coefficients $s_i^{(k)}$ and $c_i^{(k)}$ for $k = 1 \dots K$:

$$\boldsymbol{\theta} = \left(s_0^{(1)} \cdots s_{2M+1}^{(k)} c_0^{(1)} \cdots c_{2M+1}^{(k)} \right)^T, \tag{18}$$

where T stands for the transpose operator. The matrix $\boldsymbol{\Phi}$ contains the signal model specifications:

$$\boldsymbol{\Phi} = (\boldsymbol{\Phi}_1 \boldsymbol{\Phi}_2 \cdots \boldsymbol{\Phi}_K), \tag{19}$$

$$\boldsymbol{\Phi}_k = (\mathbf{S}_k \quad \mathbf{C}_k) \begin{pmatrix} \mathbf{t} \\ \mathbf{t} \end{pmatrix}, \tag{20}$$

$$\mathbf{S}_k = diag\left(\sin 2\pi f_0^{(k)} t_1 \ldots \sin 2\pi f_0^{(k)} t_N\right), \tag{21}$$

$$\mathbf{C}_k = diag\left(\cos 2\pi f_0^{(k)} t_1 \ldots \cos 2\pi f_0^{(k)} t_N\right), \tag{22}$$

$$[\mathbf{t}]_{np} = t_n^p, p = 0 \ldots P, n = 1 \ldots N. \tag{23}$$

The frequencies $f_0^{(k)}$ in (21) correspond to the K largest components in $x(t_n)$. These frequencies were found as follows: 1) $x(t_n)$, $n = 1 \ldots N$ was multiplied by the Hanning window and the zero-padded FFT was calculated; 2) in the magnitude spectrum the local maxima were found and ordered according to its strength; 3) the first K maxima were retained, together with their frequencies $f_0^{(k)}$, $k = 1 \ldots K$. Combining (16)–(23) the coefficients $\boldsymbol{\theta}$ are estimated as:

$$\hat{\boldsymbol{\theta}} = \left(\boldsymbol{\Phi}^T \boldsymbol{\Phi}\right)^{-1} \boldsymbol{\Phi}^T \mathbf{x} \approx \boldsymbol{\Phi}^+ \mathbf{x}, \tag{24}$$

with $\boldsymbol{\Phi}^+$ being the pseudoinverse of $\boldsymbol{\Phi}$. The resulting EMG time-waveform is readily obtained:

$$\hat{\mathbf{x}} = \boldsymbol{\Phi} \hat{\theta}. \tag{25}$$

III. Results, Discussion and Applications

A. EMG Signal Recordings

Surface EMG signals have been recorded from five healthy male subjects (Mean $\pm$ SD; age 30.4 ± 5.4 yr; height 171.0 ± 6.5 cm; body mass 66.4 ± 7.6 kg). The study was approved by the local ethics committee according to the Declaration of Helsinki. All the subjects were informed about the experiment and gave their written consent prior to inclusion. The signals from the vastus medialis and vastus lateralis were recorded using a grid of 5×13 electrodes (inter-electrode distance of 2.5 mm) in monopolar configuration and sampled at $f_s = 2048$ Hz (EMG amplifier, OT-Bioelettronica, Italy). After careful preparation of the skin, electrode pairs were placed longitudinally on the middle portion of the muscles. The contractions were performed in an isokinetic machine (KinCom, Chattanooga, USA). The subjects were seated on the isokinetic's chair and the rotation axis of the knee was aligned with the rotation axis of the dynamometer arm. The right leg was fixed to the dynamometer arm using velcro straps. To avoid body movements, the subjects were secured to the chair with straps across the chest and hips. Prior to the experiment two attempts of maximal voluntary contractions (MVC's) were performed. The maximal force value of the two attempts was assumed as the subject's MVC. After five minutes of rest, two isometric contractions were performed: one at 10% of MVC and the other at 50% MVC. The time rest between the contractions was 5 minutes and the duration of each contraction 1 minute.

B. EMG Signal Model Validation

The EMG signal model verification was carried out by evaluating the modeling error as a function of the analysis window

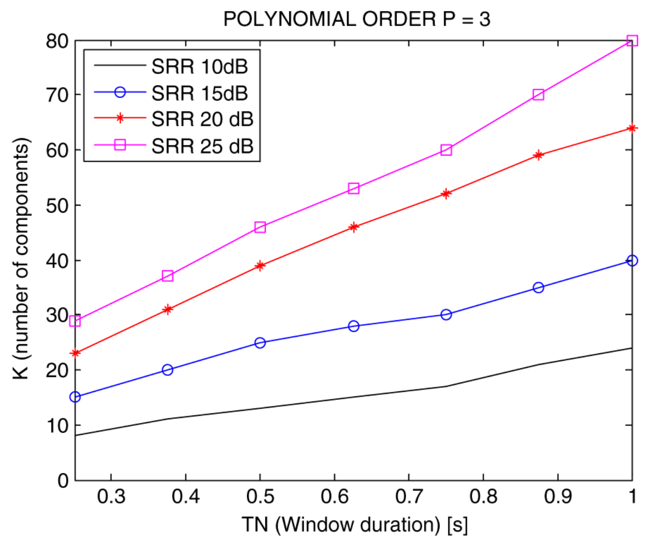

(a)

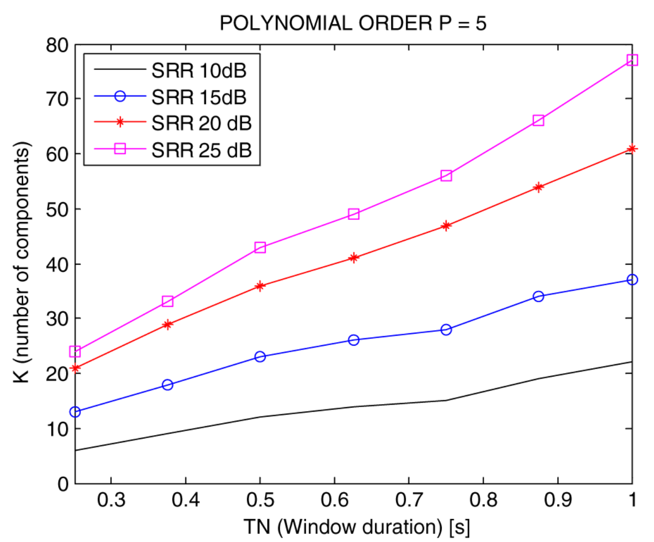

(b)

Fig. 2. Equal-SRR contours as a function of the number of components K and window duration T_N: (*a*) $P = 3$ and (*b*) $P = 5$.

duration ($T_N = N/f_s$), the number of components (K) and the model order ($P = 2M + 1$). We processed a total of $5 \times 64 \times 200000$ samples in the following way: 1) the input signals were segmented in blocks according to the chosen window size; 2) for each segment we calculated the corresponding approximation via (24) and we evaluated the modeling error by the Signal-to-Residual Ratio (SRR):

$$SRR = \left(\sqrt{\sum_{n=1}^{N} |x(t_n)|^2 / \sum_{n=1}^{N} |x(t_n) - \hat{x}(t_n)|^2}\right)_{dB}. \tag{26}$$

By varying K and P, (27) yielded a large number of outcomes from which we calculated the averages, shown in the form of equal-SRR contours for $P = 3$ and $P = 5$ in Fig. 2. These contours, conceived as a measure of K versus T_N for which the modeling error is constant, display a number of interesting features for a potential user. First it is seen that the ascending trend in all contours means that longer windows yield higher frequency resolution, which in turn generates more peaks in

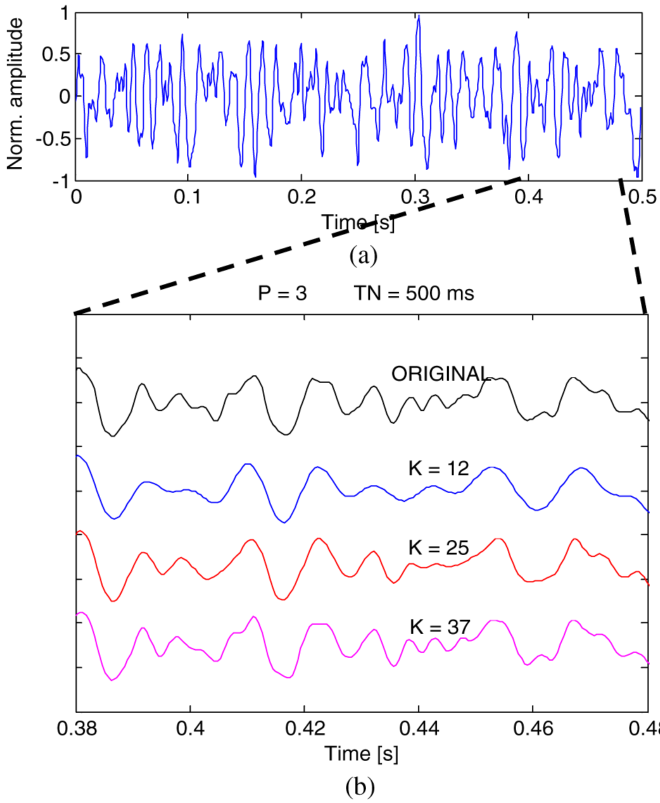

Fig. 3. (*a*) 500 ms EMG time waveform; (*b*) a zoomed segment around 430 ms (top) and the modeled segment for $K = \{12, 25, 37\}$ with $P = 3$.

the spectrum. This increase is solely due to the windowing effect i.e. a larger analysis window gives rise to a narrower spectral mainlobe and, consequently, higher frequency resolution and larger spectral component discrimination capacity. Accordingly, K must also increase in order to keep the SRR constant. Notice that the displacement between the contours is not uniform, due to the fact that the relationship between K and T_N is not necessarily linear. Also note that by increasing the model order P (compare subfigures a and b) the modeling error for each component shrinks, which means that fewer components are needed for a given SRR. In addition, Fig. 2 provides the mean for the choice on P for the given application constraints e.g. memory requirements, compression factor, maximum allowable signal distortion.

An illustration of the above argumentation is shown in Fig. 3 where a 500 ms input signal segment (shown in subfigure a) was approximated by the time-varying multicomponent model for $P = 3$ and $K = \{12, 25, 37\}$. A zoomed portion of the segment around $t = 430$ ms and the three approximations are shown in subfigure b from top to bottom. Notice that for $K = 12$ the shape of the original waveform is roughly preserved, although the fine variations are lost. In this case, the relative Mean Square Error (MSE), calculated as $\mathrm{MSE} = 10^{-\mathrm{SRR}/10}$ is 9.7%. By increasing K the approximation gets better and for $K = 37$ the modeled waveform is almost the same as the original ($\mathrm{MSE} = 0.3\%$).

The method is further evaluated by comparing its compression performance to two state-of-the art methods. The former is an embedded zero-tree wavelet decomposition, which is superior to the classical hard thresholding wavelet approach [14]. The latter combines the DWT with artificial neural networks [15]. The comparison is carried out by means of the mean SRR (dB) as a function of the compression factor $C = (L_{orig} - L_{compress})/L_{orig} \times 100(\%)$, where L_{orig} and $L_{compress}$ stand for original and compressed data length respectively. The results of the comparison are shown in Table I. Observe that for $C \leq 85\%$ the proposed method outperforms the reference methods; as C gets larger all the methods exhibit a similar performance. Hence, the time-variant multicomponent modeling approach seems to be a good candidate for EMG signal compression.

TABLE I
MEAN SRR (dB) VS. COMPRESSION FACTOR FOR THREE METHODS

Compression factor (%)	70	75	80	85	90	95
Zero-tree wavelet	26.7	26.3	25.6	21.9	16.7	11.2
DWT & neural networks	30.4	30.1	27.7	23.0	17.7	12.0
Proposed	32.6	32.2	29.8	23.8	17.5	11.9

C. Other Potential Applications

Muscle activity detection, very useful for the purpose of motor control and posture analysis, is a challenging task for a broadband noise (weak EMG responses) or in presence of spurious peaks (e.g. electrocardiogram). The proposed method provides a way to estimate onset/offset events in a muscle contraction from a single signal component by examining its estimated time-varying amplitude $\hat{A}_k(t) = \sqrt{s_k^2(t) + c_k^2(t)}$. Because $\hat{A}_k(\mathrm{t})$ is highly localized in the frequency domain, such an approach would be robust against the aforementioned perturbations and it might give a deeper insight into how different signal components respond to a specific change in muscle activity.

Muscle fibre conduction velocity estimation is often biased by the existence of the non-propagating components (resulting from the initiation and extinction of the action potential at the neuromuscular and fibre-tendon junctions respectively). For a two-channel acquisition the proposed method can be used to estimate the time delay d_k of a single signal component during the propagation along the detection grid $d_k = (\theta_k^{(1)} - \theta_k^{(2)})/2\pi f_0^{(k)}$, where $\theta_k^{(1)}$ and $\theta_k^{(2)}$ are the initial phase of the kth signal component in channel 1 and channel 2 respectively, calculated via (3). By combining the delays from all K components we can obtain a time-delay estimation of a/the non-uniform signal propagation, which is characteristic of surface EMG signals. Moreover, the components with delays smaller than the lower physiological limit [22] can be classified as non-propagating and removed from the signal model, thus reducing the bias in conduction velocity estimates.

IV. CONCLUSIONS

We have shown that time-variant multicomponent signal modeling is an adequate approach for representing surface EMG waveforms. As a compression tool, it outperforms two wavelet-based methods for compression factors up to 85%. In addition, we believe that the proposed approach can fit well into applications related to onset/offset detection and conduction velocity estimation.

References

[1] R. Merletti, M. Knaflitz, and C. J. De Luca, "Myoelectric manifestations of fatigue in voluntary and electrically elicited contractions," *J. Appl. Physiol.*, vol. 69, no. 5, pp. 1810–1820, Nov. 1990.

[2] G. F. Inbar and A. E. Noujaim, "On surface EMG spectral characterization and its application to diagnostic classification," *IEEE Trans. Biomed. Eng.*, vol. 31, no. 9, pp. 597–604, Sep. 1984.

[3] O. Paiss and G. F. Inbar, "Autoregressive modeling of surface EMG and its spectrum with applications to fatigue," *IEEE Trans. Biomed. Eng.*, vol. 34, no. 10, pp. 761–770, Oct. 1987.

[4] T. Kiryu, C. J. De Luca, and J. Saitoh, "AR modeling of myoelectric interference signals during a ramp contraction," *IEEE Trans. Biomed. Eng.*, vol. 41, no. 11, pp. 1031–1038, Nov. 1994.

[5] R. Merletti and L. R. Lo Conte, "Advances in processing of surface myoelectric signals: Part 1," *Med. Biol. Eng. Comput.*, vol. 33, no. 3, pp. 362–372, May 1995.

[6] S. Karlsson and J. vu, "Estimation of surface electromyogram spectral alteration using reduced-order autoregressive model," *Med. Biol. Eng. Comput.*, vol. 38, no. 5, pp. 520–527, Sep. 2000.

[7] E. S. G. Carroti, J. C. de Martin, D. Farina, and R. Merletti, "Linear predictive coding of myoelectric signals," in *Int. Conf. Acoust. Speech and Sig. Proc.*, Philadelphia, PA, USA, Mar. 2005, vol. 5, pp. 629–632.

[8] G. Yang, S. Wang, and Y. Chen, "SEMG analysis basing on AR model and Bayes taxonomy," *Appl. Mech. Mater.*, vol. 44-47, pp. 3355–3359, Dec. 2011.

[9] Z. O. Khokhar, Z. G. Xiao, and C. Menon, "Surface EMG pattern recognition for real-time control of a wrist exoskeleton," *BioMed. Eng. Online*, vol. 41, no. 9, Aug. 2011, 10.1186/1475-925X-9-41.

[10] H. Kato, M. Taniguchi, and M. Honda, "Statistical analysis for multiplicatively modulated nonlinear autoregressive model and its applications to electrophysiological signal analysis in humans," *IEEE Trans. Biomed. Eng.*, vol. 54, no. 9, pp. 3414–3425, Sep. 2006.

[11] E. J. Scheme, B. Hudgins, and P. A. Parker, "Myoelectric signal classification for phoneme-based speech recognition," *IEEE Trans. Biomed. Eng.*, vol. 54, no. 4, pp. 694–699, Apr. 2007.

[12] K. Lee, "EMG-based speech recognition using hidden markov models with global control variables," *IEEE Trans. Biomed. Eng.*, vol. 55, no. 3, pp. 930–940, Mar. 2008.

[13] J. Chiang, Z. J. Wang, and M. J. McKeown, "A hidden markov, multivariate autoregressive (HMM-mAR) network framework for analysis of surface EMG data," *IEEE Trans. Biomed. Eng.*, vol. 56, no. 8, pp. 4069–4081, Aug. 2008.

[14] J. A. Norris, K. B. Englehart, and D. F. Lovely, "Myoelectric signal compression using zero-trees of wavelet coefficients," *Med. Eng. Phys.*, vol. 25, pp. 739–46, 2003.

[15] P. A. Berger, F. A. O. Nascimento, J. C. Carmo, and A. F. Rocha, "Compression of EMG signals with wavelet transform and artificial neural networks," *Physiol. Meas.*, vol. 27, no. 6, pp. 457–465, Jun. 2006.

[16] L. Brechet, M. Lucas, C. Doncarli, and D. Farina, "Compression of biomedical signals with mother wavelet optimization and best-basis wavelet packet selection," *IEEE Trans. Biomed. Eng.*, vol. 54, no. 12, pp. 2186–2192, Dec. 2007.

[17] Y. Stylianou, "Applying the harmonic plus noise model in concatenative speech analysis," *IEEE Trans. Speech Audio Process.*, vol. 9, no. 1, pp. 21–29, Jan. 2001.

[18] R. Badeau, B. David, and G. Richard, "High-resolution spectral analysis of mixtures of complex exponentials modulated by polynomials," *IEEE Trans. Signal Process.*, vol. 54, no. 4, pp. 1341–1350, Apr. 2006.

[19] M. Zivanovic and J. Schoukens, "Single and piecewise polynomials for modeling of pitched sounds," *IEEE Trans. Audio, Speech Lang. Process.*, vol. 20, no. 4, pp. 1270–1281, May 2012.

[20] R. Merletti, "Standards for reporting EMG data," *J. Electromyography Kinesiology*, vol. 1, no. 9, pp. III–IV, Feb. 1999.

[21] L. Cohen, *Time-Frequency Analysis*. Upper Saddle River, NJ, USA: Prentice-Hall, 1995.

[22] K. C. McIntosh and D. A. Gabriel, "Reliability of a simple method for determining muscle fiber conduction velocity," *Muscle Nerve*, vol. 45, no. 2, pp. 257–265, Feb. 2012.